

IMPROVEMENT IN PRECISION OF SEDIMENTATION-EQUILIBRIUM EXPERIMENTS WITH AN ON-LINE ABSORPTION SCANNER

Robley C. WILLIAMS Jr.

Department of Biology, Yale University, New Haven, Connecticut 06520, USA

An on-line computerized optical absorption scanner for the analytical ultracentrifuge has been developed and tested. It makes direct use of the instantaneous photomultiplier output, which is digitized and averaged by the computer. It incorporates a stepping motor to drive the photomultiplier, two analog-to-digital converters, and a device which monitors precessional movement of the rotor. The scanner has been employed chiefly in sedimentation equilibrium experiments, and techniques have been devised to correct for the adverse effects of inhomogeneities of apparent absorbance which arise from the cell windows. Correction for rotor movements which occur during the scan is also possible. The completed apparatus is a successful one, and provides a significant improvement in precision, speed and convenience over the commercially available scanners. The limitations on precision inherent in the present design are examined, and it is concluded that the combined effects of window inhomogeneities and rotor movement lead to uncertainty of the measured absorbance which is unlikely to be reduced below ± 0.001 A.

1. Introduction

Optical absorption scanning systems for the ultracentrifuge [1, 2] have met with wide success, and commercial versions of such systems are available. A number of scanning systems have been built in which computers are utilized to carry out many of the data-gathering and control functions [3–9]. Such a system is described here. It was designed primarily for sedimentation equilibrium measurements, with precision rather than speed of operation as its primary goal. The performance of the system is analyzed, in order to clarify some of the present limits to precision of measurement of optical absorption in the ultracentrifuge.

2. Considerations of technique

In order to maximize precision of measurement with any absorption scanner, it is necessary to correct the absorbance data obtained in an experiment for the “baseline” of apparent absorbance that can be observed from a water-filled ultracentrifuge cell. Such baseline corrections are commonly made when refrac-

tometric optical systems are employed [10], but they have seldom been reported in measurements with the absorption scanner. A primary cause of these baseline irregularities is deposition of foreign material (oil, dust, etc.) on the windows of the cell. With the customary demountable cells [10], the windows must be cleaned each time the cell is filled. If one attempts to measure the baseline after such cleaning, much of the detailed perturbation of the absorbance is lost. However, equilibrium cells have been designed [11] which do not have to be taken apart between runs, and such “external loading” cells make good baseline correction possible. In routine sedimentation equilibrium experiments, therefore, we carry out the experimental run and then immediately remove the cell, extensively rinse the solution channels, and then refill them with solvent. We then carry out measurements of the apparent absorbance of this blank cell under conditions identical to those of the experimental run. The absorption baseline so obtained is subtracted from the experimental points as indicated in fig. 1. The correction of small irregularities which can be achieved by subtraction of the baseline is apparent, and the increase in precision obtainable through such correction has

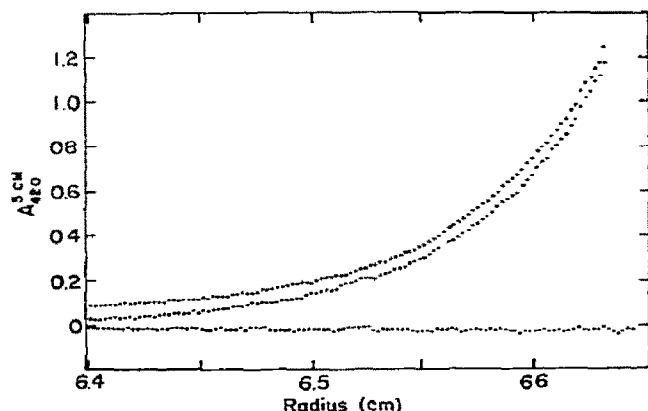


Fig. 1. Sedimentation equilibrium of CO-hemoglobin A, at 20,000 rpm in a cell [11] of 30 mm optical path. Measurements made with the scanner described in this paper. The lower curve shows the cell baseline obtained after the experiment; the middle curve shows the experimental data; the upper curve (displaced upward by 0.05 A for clarity) shows the experimental data after correction by subtraction of the cell baseline. (See text for details of technique.) Conditions: monochromator slit at 0.8 mm; photomultiplier slit at 0.08 mm; image focussed near the $\frac{2}{3}$ -plane of the cell.

been a primary influence in the design of the present scanner system.

3. Apparatus

The apparatus presently in use in our laboratory is schematically described in fig. 2. It is based on the commercially available Beckman Model E scanner (Beckman Instrument Co., Palo Alto, Calif.). The standard photomultiplier was retained, together with its housing, lead screw, and power supply. The monochromator and Hg-Xe lamp were also retained. In operation, the pulses of voltage produced by the photomultiplier when the cell passes through the light beam are acquired at the "sampler output" jack on the scanner, and the rotor-collar timing marks are acquired at the two "Schmitt trigger" jacks on the multiplexer. Both the photomultiplier output and the timing pulses are buffered and passed to the acquisition computer, a PDP-8/E (Digital Equipment Corp., Maynard, Mass.) equipped with 16K of core memory, two analog-to-digital converters, and a digital input-output module. Several of the special elements of design incorporated into this system are discussed below.

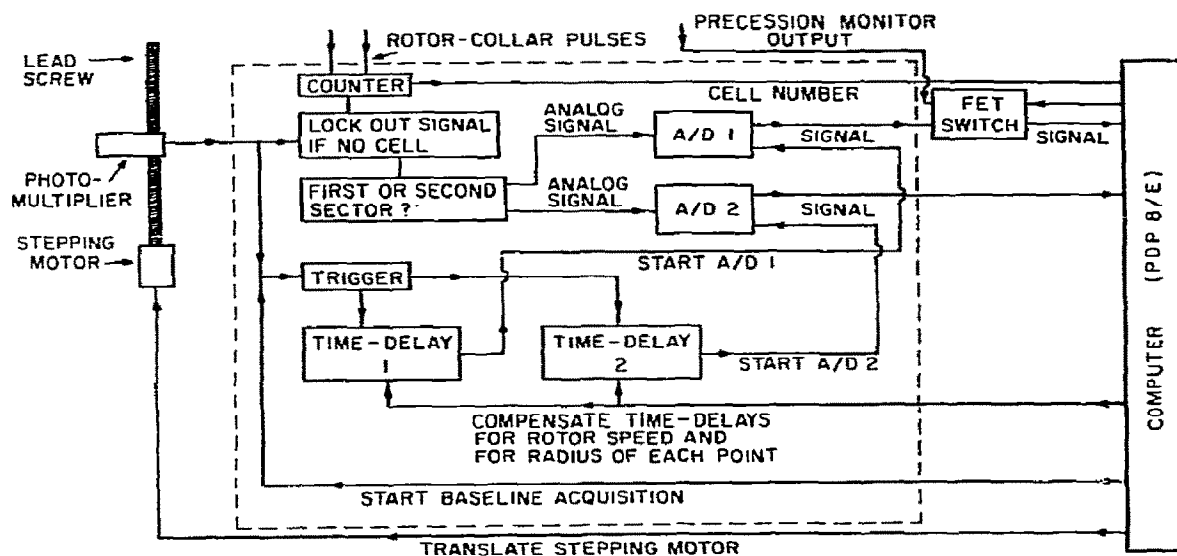


Fig. 2. Schematic diagram of absorption scanner functions. The interface (within dashed lines) between the photomultiplier output and the digital computer was constructed of packaged digital modules ("Flip-Chip", Digital Equipment Corp., Maynard, Mass.) at a cost of about \$1500. A detailed schematic diagram is available from the author upon request.

3.1. Stepping motor

A stepping motor [12] (SLO-SYN, Model HS-25, Superior Electric Co., Bristol, Conn.), geared down 12:1, drives the photomultiplier lead screw under computer control. (The gear reduction provides about 7400 steps between the counterweight edges: one step corresponds to about 2.2 microns in the cell.) This arrangement, similar to that described by Cohen [7], has numerous advantages over the dc motor usually employed to drive the lead screw. First, reproducible positioning of the photomultiplier can be achieved, so that cell baseline corrections are relatively simply and reliably done. Second, the photomultiplier can "dwell" at any given radial position for a variable length of time, determined by the program, in order to reduce the signal-to-noise ratio below a preset value [3]. Third, the radial spacing can be varied by the program to be large in regions of shallow gradient and small in regions of steep gradient.

3.2. Timing of signal acquisition

For reasons set forth below, the timing of sample acquisition is a delicate problem. Fig. 3 shows the response of the stationary photomultiplier as one channel of a cell passes before it. The top region of the pulse is seen to be not completely flat; but rather it shows ripples. The ripples are the circumferential counterpart of the radial irregularities apparent in the baseline scan in fig. 1. They have at least three sources: deposition of oil and other foreign material on the windows of the cell, absorbing or refracting inhomogeneities in the windows themselves, and reflections from the side walls of the centerpiece which are the unavoidable consequence of poor collimation of the light from the monochromator. Since absorbance is inferred from the voltage at the top of the pulse, it is important to control and reproduce the *circumferential* position at which this voltage is acquired (hence its timing) as well as the *radial* position. If the timing of acquisition is not reproducible between the experimental run and the baseline run, good correction cannot be expected.

In order to obtain precisely reproducible timing, the following strategy has been adopted. The cell is filled in such a way that the first light-pulse encountered is from the solvent, and the second is from the

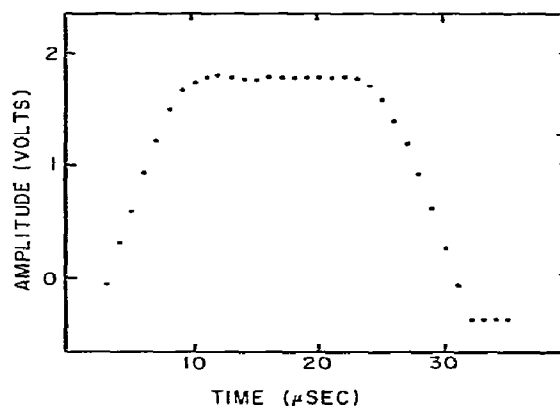


Fig. 3. Profile of a pulse from the photomultiplier. The photomultiplier was held stationary, and its output was acquired with a 400 ns window, at the delay times shown on the horizontal axis. Each point represents the mean of 400 revolutions of the rotor at a given delay time, and the uncertainty on the vertical axis is smaller than the diameter of the points. (The "ripple" in the flat region at the top of the pulse is typical of that seen at other radial positions, although the shape varies from one position to another.) Conditions: wavelength of 546 nm, monochromator slit at 2.0 mm, photomultiplier slit at 0.08 mm.

solution. This "backward" loading causes the leading edge of the first pulse to be reproducible, at a given radius, between the experimental and baseline runs. The leading edge of the solvent pulse is employed to trigger two time-delay circuits (see fig. 2). Since the slits over the cell are parallel rather than radial, the time elapsed from the occurrence of the trigger to the center of a pulse becomes markedly shorter as radius increases. To compensate, a 2 MHz crystal clock and counter have been incorporated into the interface to adjust the delay time. The delay is recalculated by the program each time the radius is altered, and the counter is set appropriately. In this way acquisition times can be obtained which are reproducible to better than 0.1 microsecond between the experimental run and the baseline run. With such reproducible timing, and with the use of externally loaded cells, the effects of circumferential inhomogeneities of the windows are minimized.

3.3. A/D converters

Two analog-to-digital converters are employed

(fig. 2), so that *both* the sample pulse and the solvent pulse can be acquired in the same pass of the rotor. This design saves time, and it has the additional advantage of reducing the effect of low-frequency fluctuations in light intensity which are present in the output of the Hg—Xe lightsource. The drawback is that the converters must be calibrated periodically to insure that they perform identically with respect to gain. Differences in zero offset between the two converters are compensated by sampling the photomultiplier dark response during each revolution with each converter, and subtracting these dark values from the measured values of the light pulses.

3.4. Precession monitor

A usually unknown but potentially large source of measurement error arises from movements of the rotor with respect to the optical bench. Such movements, chiefly manifest as precession, are generally slow, with periods in the range 2–40 seconds, and can often be described as oscillations driven by building motion, by imperfections in the drive unit, or by both. Amplitudes of these movements vary, but can be as great as 50 microns. The slowness of the movements makes them of relatively little consequence in interferometric measurements, where the whole cell is measured at once, and where pulsed laser measurements [13] can yield a complete interference pattern in a single pass of the rotor. However, the scanner dwells typically for 0.2 to 2.0 seconds at one position in the image and is then moved to the next. Therefore, the radial position to be assigned to a given location of the photomultiplier is uncertain by the amount of the precessional amplitude. The uncertainty can have large effects: for example, for a gradient of 20 A/cm (corresponding to a value of $d(\ln c)/d(r^2/2)$ of about 3 cm^{-2} and an absorbance of 1.0), displacement of the rotor by ± 10 microns yields an uncertainty of 0.02 A in the final data. Observation in our own data and in those of others [6] of unexpectedly large deviations at high concentration gradients led to construction of a precession monitor.

A sketch of this monitor is shown in fig. 4. A magnetic proximity probe (Model 190-F, Bentley-Nevada Co., Minden, Nev.) is held by means of a swing-out arm on the rotor support fork at a distance of about 2 mm from the rotor collar. This probe, driven by an

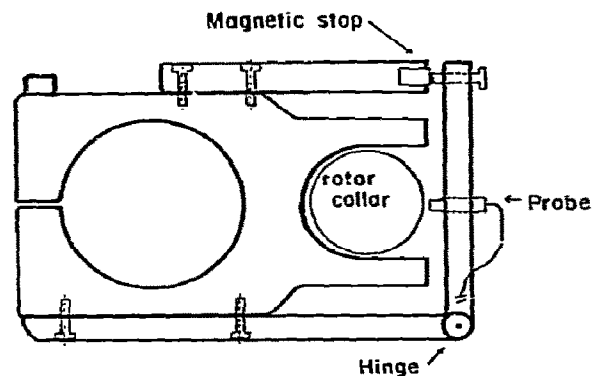


Fig. 4. Sketch of the rotor precession monitor. The Model E rotor support fork is shown, and the position of the rotor collar is indicated. The magnetic stop is provided as a safety device in case large excursions of the rotor should occur. Adjustment of the distance between collar and probe is made with the screw which bears against the stop. The electrical leads from the probe are passed out of the vacuum system via unused terminals on the feedthrough supplied with the multiplexer.

appropriate oscillator and rectifier circuit (Model 3106, Bentley-Nevada Corp.) provides a DC potential which varies linearly with the distance of the rotor collar from it. In operation, the photomultiplier dwells at a given point in the image and a number of light pulses are acquired. Halfway through this process, an FET switch (see fig. 2) is activated by the program, and the output of the detector circuit, amplified and smoothed, is routed to one of the analog-to-digital converters. The voltage obtained is used to correct the radius at the given point.

The monitor is calibrated by observing a meniscus image with the photomultiplier stationary, as shown in fig. 5. In fig. 6, rotor movement is shown under two sets of conditions. At the top is shown the displacement with time of the stationary rotor, which is of relatively high frequency (approximately 2 Hz) and reflects the behavior of the rotor as a pendulum driven by the vibration of the building. At the bottom is shown the low frequency (approximately 0.08 Hz) motion of the rotor at 20 000 rpm. The amplitude shown (± 5 microns) is typical of the behavior of the relatively heavy An-E rotor over a range of moderate speeds. As noted by Yphantis [10], however, the amplitude of low frequency precessional motion of the

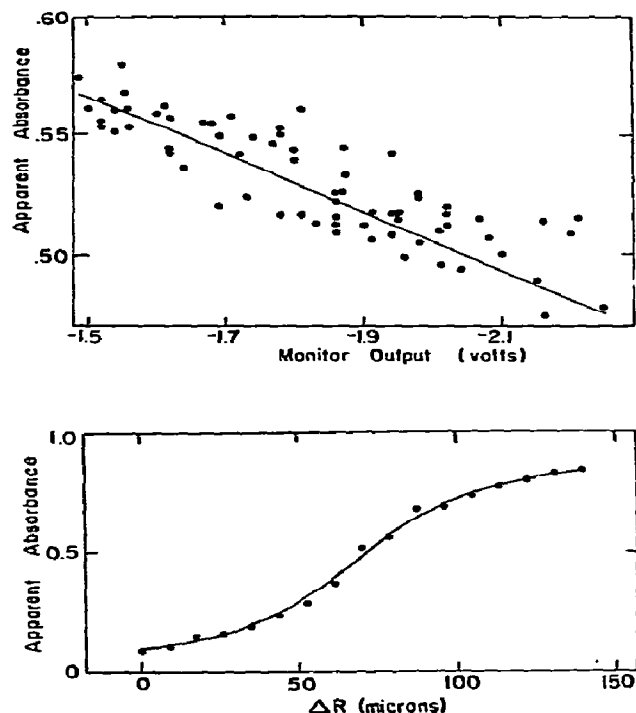


Fig. 5. Calibration of the precession monitor. A solution of large absorbance (near 2) is placed in the sample channel. The photomultiplier is stopped at a point in the meniscus image of the solution, and simultaneous recording is made of the apparent absorbance and of the output of the precession monitor (top). Afterward, the meniscus image is scanned repeatedly (bottom), and a calibration of output vs radius is arrived at by combination of the two curves.

rotor varies greatly with such variables as the nature of an individual drive unit, the levelling of the drive and the mass of the rotor.

4. Results

The actual performance of this system can be assessed in several ways, in order to illuminate the problems which still limit absorption optical systems for the ultracentrifuge. As a signal averaging device, the scanner behaves properly. Fig. 7 shows a plot of the reciprocal of the standard deviation about the mean as a function of the square root of the number of

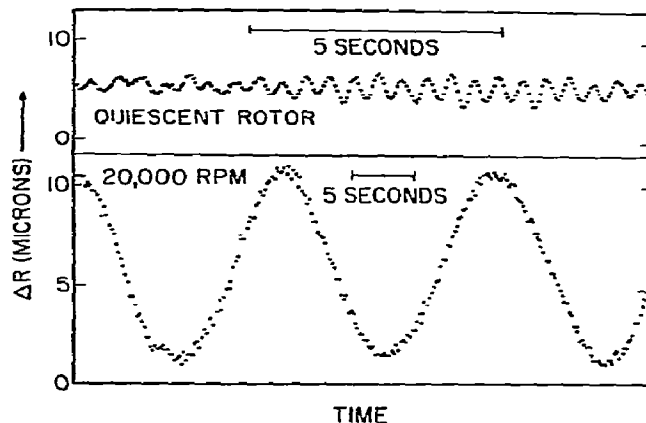


Fig. 6. Rotor movements observed with the precession monitor. (Top) Rotor not running, rotor-chamber closed, pumps off. (Bottom) Type An-E rotor running at 20 000 rpm. The vertical coordinate (ΔR) refers to displacements of the centrifuge cell with respect to the optical bench.

pulse-pairs averaged in each of 50 trains of pulses. The relationship shows the expected linearity. When 400 pulse-pairs are averaged under conditions of bright illumination, a standard deviation near ± 0.0005 A is obtained. As the monochromator slit is narrowed, however, the precision falls. The performance of the system is therefore limited in the first instance by the

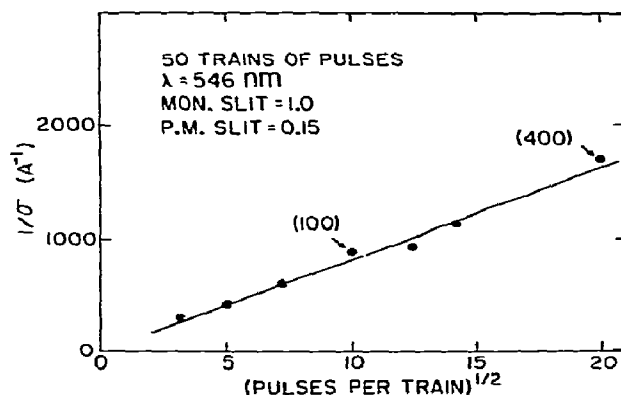


Fig. 7. Signal-averaging behavior of the scanner. Fifty trains of pulse-pairs were acquired, with different numbers of pulses per train in each group of 50 trains. The standard deviation (σ) about the mean was computed for each group of trains. Conditions as indicated.

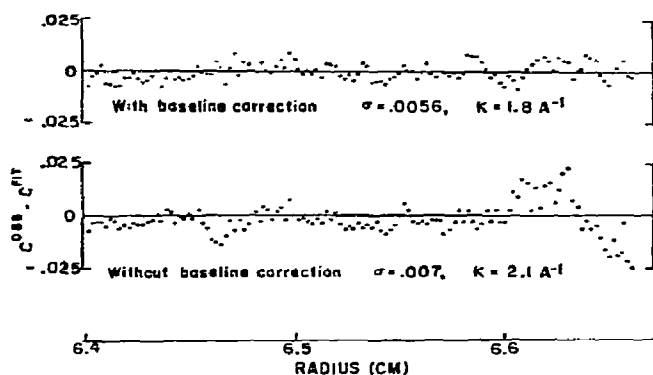


Fig. 8. Residuals about the best-fitting dimer-tetramer relationship. CO-hemoglobin A at sedimentation equilibrium at 20 000 rpm, 20°C, in an "external loading" cell of 30 mm optical path. The scale of the vertical axis is absorbance in a 3 cm path (see text for details). Conditions: wavelength of 420 nm, monochromator slit at 0.8 mm, photomultiplier slit at 0.08 mm, 400 pulse-pairs/point.

intensity of the light available from the monochromator.

The strategy of cell-baseline correction is a useful one in improving precision, as indicated in fig. 2. A more graphic illustration is shown in fig. 8. Data from a single channel of CO-hemoglobin A are plotted at sedimentation equilibrium. A fit was carried out to yield the best dimer-tetramer equilibrium constant, and the residuals about the fitting function (concentration vs. radius) are shown as a function of radius. It is apparent, both from the shapes of these residual curves and from the standard deviations about the fitting function, that the baseline correction improves the precision of the fit. The value of the observed association constant is also modified by the baseline correction.

The effect of correction of the radial coordinate data for rotor movement is shown in fig. 9. Two scans were taken in succession at sedimentation equilibrium from a solution of CO-hemoglobin S. The first scan was subtracted from the second. In the upper curve, the subtraction was performed after the radii had been corrected for rotor movement by use of the precession monitor. In the lower curve, no radial correction was applied before the subtraction of the same two scans. Two effects are apparent. First, the radial correction markedly improves the overall reproducibility of the

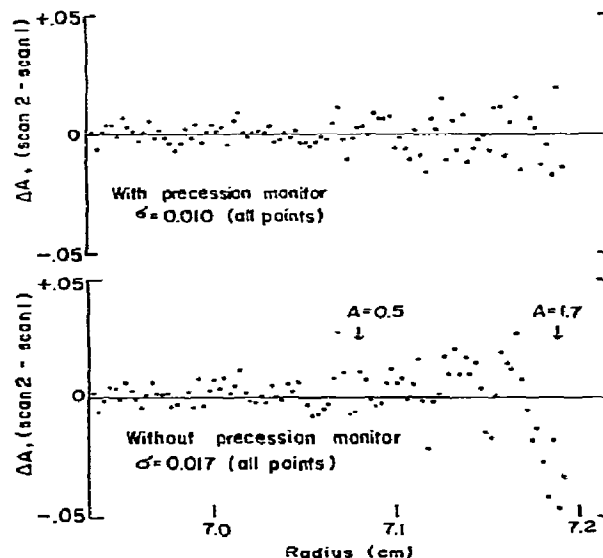


Fig. 9. Difference between two successive scans of the same sedimentation equilibrium distribution (Top) Difference corrected for movement of the rotor. (Bottom) Uncorrected difference. The standard deviations of the differences (σ) are indicated. Conditions as in fig. 8. (See text for details.) 200 pulse-pairs/point.

data from one scan to the next. Second, the improvement is most pronounced at large gradients, as one would expect, although even with the correction precision tends to be lost as the gradient increases (see below).

5. Conclusions

The computerized absorption scanner described here is a satisfactory instrument, and has been used routinely for about six months to measure subunit association in hemoglobins. When employed with externally loaded cells and with the technique described, sufficient precision is obtained to measure the dimer-tetramer association constants of various hemoglobins with a reproducibility near 10%. Although comparison is difficult because of differences in the techniques employed with each scanner, it seems safe to assert that an improvement in precision by a factor of at least two has been made over that obtained with the standard Model E scanner. In addition, speed and con-

venience are gained because of the fact that the data obtained are already stored in the computer, ready for analysis without the necessity of numerical manipulation. The most useful points to be made, however, deal not with the successes of the design, but with its limitations.

Under practical operating conditions, the precision of the scanner lies in the region of ± 0.003 A to ± 0.010 A. The primary limitation appears to arise directly from the low intensity of the light available from the DU monochromator and 100 watt Hg-Xe lamp. Some improvement in precision could be obtained by the use of a more intense light source (such as the laser described briefly by Crepeau et al. [8, 14]) while averaging a practical number (hundreds) of pulse-pairs.

Even with sufficient light intensity, however, the effective inhomogeneity of the cell windows, in both the radial and circumferential directions, provides a limitation of a second kind to the precision obtainable. The irregularities of baseline absorbance (fig. 1) can be partially corrected by subtraction. A full correction, however, seems to be difficult to achieve for at least two reasons. The first is the steeply varying nature of the irregularities. For example, two neighboring points in a baseline scan, at a radial spacing of 20 microns, frequently differ in apparent absorbance by 0.01 A. An uncertainty of 10 microns in rotor position within such a small region leads to an uncertainty of ± 0.005 A in the baseline absorbance assigned at that radius. A second reason for incomplete correction of baseline irregularities appears to be that some of them arise not from inhomogeneity of the windows, but from reflections from the side walls of the cell. With sufficiently precise timing, reflections originating in the reference channel of the cell will be well reproduced between the experimental and baseline runs. Reflections originating in the sample channel are, however, partly absorbed by the sample, and are therefore not reproducible between the two runs. The reflections are the result of poor collimation of light from the monochromator of the Model E. The only remedy for them would seem to be a better collimated light-source.

Rotor movement presents particular difficulties to the absorption scanner because of the fact that the photomultiplier moves slowly with respect to the rate of precession and is exposed to only part of the image

at any given time. *Complete* correction for rotor movement is not possible, even with the rather precise precession monitor described above. The incompleteness is due to the fact that the monitor must assign a unique radius to the mean of several hundred pulse-pairs, acquired over 0.2 to 2.0 seconds. During that time, the rotor can swing a significant distance. For instance, the data taken for fig. 8 represent means of 200 pulse-pairs taken over 0.6 seconds. The rotor was moving approximately as shown in fig. 6, and the uncertainty in its position over the time of acquisition was as great as 1.5 microns.

The problems of rotor movement are most severe where the gradient of absorbance is large (fig. 9). However, since large gradients of absorbance due to window inhomogeneities exist everywhere in the cell, partial correction for rotor movement by the methods described above seems likely to leave residual uncertainties of the order of ± 0.001 A in the absorbance assigned to a given radius in the cell. No amount of signal averaging will remove them. Future scanner designs could be greatly improved by providing for complete recording and radial correction of the image of the whole cell at each revolution of the rotor. The "optical multichannel analyzer" of Richards and co-workers [15] seems to be a step in that direction, although it is still constrained by the necessity to average several revolutions before it can be read.

Acknowledgement

This work was supported by Grant HL 12901 of the National Institutes of Health. Much of the interface was designed and built by Mr. Walter S. Lund. Dr. David Yphantis contributed both discussion and parts to the construction of the precession monitor, and also much helpful discussion of other aspects of the apparatus described. Able technical assistance was provided by Ms. Helen Kim.

References

- [1] S.P. Spragg, S. Travers and T. Saxton, *Anal. Biochem.* 12 (1965) 259.
- [2] H.K. Schachman and S.J. Edelstein, *Biochemistry* 5 (1966) 2681.

- [3] S.P. Spragg and R.F. Goodman, *Ann. N.Y. Acad. Sci.* 164 (1969) 294.
- [4] A.H. Pekar, R.E. Weller and B.H. Frank, *Anal. Biochem.* 42 (1971) 516.
- [5] R.H. Crepeau, S.J. Edelstein and M.J. Rehmar, *Anal. Biochem.* 50 (1972) 213.
- [6] R.H. Crepeau, C.P. Hensley, Jr. and S.J. Edelstein, *Biochemistry* 13 (1974) 4860.
- [7] R. Cohen, *Biophys. Chem.* 5 (1976) 77.
- [8] R.H. Crepeau, R. Conrad and S.J. Edelstein, *Biophys. Chem.* 5 (1976) 27.
- [9] S.P. Spragg, W.A. Barnett, J.K. Wilcox and J. Roche, *Biophys. Chem.* 5 (1976) 43.
- [10] D.A. Yphantis, *Biochemistry* 3 (1964) 297.
- [11] A.T. Ansevin, D.E. Roark and D.A. Yphantis, *Anal. Biochem.* 34 (1970) 237.
- [12] D.E. Wampler, *Anal. Biochem.* 44 (1971) 528.
- [13] C.H. Paul and D.A. Yphantis, *Anal. Biochem.* 48 (1972) 588.
- [14] R.H. Crepeau, R. Conrad and S.J. Edelstein, *Fed. Proc., Fed. Amer. Soc. Exp. Biol.* 32 (1973) 662.
- [15] D.L. Rockholt, C.R. Royce and E.G. Richards, *Biophys. Chem.* 5 (1967) 55.